Molecular Crystals and Liquid Crystals

ISSN: 1542-1406 (Print) 1563-5287 (Online) Journal homepage: http://www.tandfonline.com/loi/gmcl20

Nanomesh Aluminum Films for LC Alignment. Theoretical and Experimental Modeling

A. K. Dadivanyan, V. V. Belyaev, D. N. Chausov, A. A. Stepanov, A. G. Smirnov, A. G. Tsybin & M. A. Osipov

To cite this article: A. K. Dadivanyan, V. V. Belyaev, D. N. Chausov, A. A. Stepanov, A. G. Smirnov, A. G. Tsybin & M. A. Osipov (2015) Nanomesh Aluminum Films for LC Alignment. Theoretical and Experimental Modeling, Molecular Crystals and Liquid Crystals, 611:1, 117-122, DOI: 10.1080/15421406.2015.1030196

To link to this article: http://dx.doi.org/10.1080/15421406.2015.1030196

Published online: 06 Jul 2015.

Mol. Cryst. Liq. Cryst., Vol. 611: pp. 117–122, 2015

ISSN: 1542-1406 print/1563-5287 online
DOI: 10.1080/15421406.2015.1030196

Nanomesh Aluminum Films for LC Alignment. Theoretical and Experimental Modeling

A. K. DADIVANYAN,[1] V. V. BELYAEV,[1,3,*] D. N. CHAUSOV,[1,*] A. A. STEPANOV,[2] A. G. SMIRNOV,[2] A. G. TSYBIN,[2] AND M. A. OSIPOV[4]

[1]Education & Research Lab of Theoretical and Applied Nanotechnology, Moscow Region State University, Moscow, Russia
[2]Belarusian State University of Informatics and Radioelectronics, Belarus, Minsk
[3]People's Friendship University of Russia, Moscow, Russia
[4]Department of Mathematics, University of Strathclyde, Glasgow, United Kingdom

A porous system for LC alignment is reviewed. Fabrication of nanomesh aluminum films and their porous structure are described. Methods of the nanomesh parameters for optimal LC alignment are discussed. A model of the LC alignment in a porous system is proposed. The LC orientation type is determined by the free anchoring energy and the micropore diameter. The difference between planar and homeotropic anchoring energies appears to be lower than the interaction energy by two orders of magnitude.

Keywords liquid crystal alignment; anchoring; nanomesh

1. Introduction

An opportunity of LC alignment by substrates with porous surface has been demonstrated in [1–5]. Such substrates contain high-purity aluminum layers treated by anodic oxidation process which form porous structures of aluminum oxide Al_2O_3. Beyond the field of LC alignment they can be used as transparent electrodes [2,6,7], antireflective coatings [8] and light emitting devices [9]. The type of LC alignment depends on the pores' size and LC anchoring [7,10].

Design and fabrication of LCD elements with nanomesh alumina structure are presented in [3,4,10,11]. Various types of NLC alignment on the nanomesh alumina films are presented in Table 1 for the orientation component of the anchoring energy ranged between 10^{-6} J m^{-2} and 10^{-2} J m^{-2} like in [12] and pore diameter from 50 nm to 250 nm [8].

Theoretical modelling of the LC alignment is well developed for flat surfaces. For example LC alignment on carbon, polyethylene and polyorganosiloxane has been simulated in [13–16]. Three components of the interaction energy of the mesogen molecules with the orienting substrate have been calculated theoretically: specific surface interaction

*Address correspondence to V. V. Belyaev and D. N. Chausov, Education & Research Lab of Theoretical and Applied Nanotechnology, Moscow Region State University, Moscow, Russia. E-mail: vic_belyaev@mail.ru; d.chausov@yandex.ru

Table 1. Various types of NLC alignment on the nanomesh alumina films

Pores diameter \ Anchoring energy (J/m^2)	50 nm	100 nm	150 nm	200 nm	250 nm
$1{\cdot}10^{-2}$	planar	planar	planar	planar	planar
$1{\cdot}10^{-4}$	vertical	vertical	tilted	tilted	planar
$1{\cdot}10^{-6}$	vertical	vertical	vertical	vertical	tilted

energy (total interaction energy) $\sim 4^{*}10^{-2}$ J m^{-2}, polar orientation energy $\sim 5^{*}10^{-4}$ J m^{-2}, azimuthal orientation energy $\sim 5^{*}10^{-5}$ J m^{-2}. As to porous systems a set of models was reviewed in [17].

One notes, however, that the physical mechanism of this effect is not clear. In this paper we present a theoretical model of the alignment for different pores.

2. Fabrication of Nanomesh Alumina Films for LC Alignment

We have selected the technology of electrochemical anodizing of thin aluminum films as the major technology of producing nanomesh aluminum films since it enables one to produce self-organizing hexagonal-packed nanostructures without using lithographic processes. The analysis of experimental results enables one to determine the relationship between the cell size D_c of the nanomesh aluminum film and anodizing voltage U. Thus, if one measures and calculates the average cell sizes of nanomesh aluminum films and correlates them with corresponding voltages which are applied while the nanomesh aluminum films are produced in different electrolytes, one obtains a linear relationship which shows that the cell size D_c of the nanomesh aluminum films is directly proportional to the applied voltage $D_c = 2.5U$. The linear relationship between the cell size and the anodizing voltage enables one to control the morphology of the structure.

The analysis of experimental results reveals the opportunity to produce self-organizing nanomesh aluminum films with specific cell sizes D_c of 50–600 nm by means of controllable electrochemical anodizing of aluminum nanomesh with the thickness over 200 nm which is followed by the selective etching of Al_2O_3.

Other characteristic parameters of the nanomesh aluminum film include the pores diameter D_p, maximum thickness $H_{\max}$, minimum thickness $H_{\min}$ and the width $L_{\min}$ of the aluminum nanomesh (Figure 1). By controllable completion of anodizing after selective etching of porous oxide an aluminum film acquires nanomesh morphology with different fill factor f, that also characterizes the nanomesh film and is determined as the ratio of the pore area S_{D_p} to the cell area S_{D_c}.

To determine the relationship between characteristic parameters of the nanomesh aluminum film and the time of its formation we have preset its morphology by means of hollow hemispheres with dense hexagonal packing which are located in the aluminum film. The thickness of the aluminum film equals the radius of the hemisphere. Figure 1 shows a schematic image of the morphology of the nanomesh film.

This model depicts a cartoon of the structure "porous alumina - aluminum" at the moment when the barrier layer touches upon the substrate. The further anodizing process

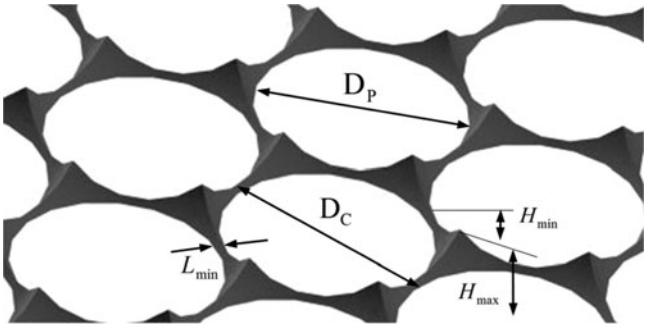

Figure 1. Schematic image of morphology of a nanomesh aluminum film.

corresponds to the movement of hemispheres below their preset radius and distance between them. Methods of control of the parameters listed above are described in detail in [18, 19].

For example, the time of forming of the nanomesh aluminum films ranges from 25 to 300 *s* and is determined by the cell size. This time range is adaptable to streamlined production and sufficient for controllable and reproducible production of nanomesh aluminum films with the preset fill factor. As shown in Table 1 and the simulation below the pore diameter influences strongly on the LC orientation type.

3. Theory of LC Alignment in Micro- and Nanopores' System

If the orientation component of the anchoring energy is small (i.e. $\Delta G \approx 10^{-6}\text{J/m}^2$) the LC alignment in the pores with diameter up to 200 nm is homeotropic. Experiments with analog models have confirmed the homeotropic alignment if the LC does not interact with the micropore surface and the pore diameter is of order of the LC cluster size. The cluster is a group of the molecules that are reoriented together under action of both electric and magnetic field. Linear size of the cluster is of the order of the coherence length.

Therefore the maximum cluster diameter is approximately equal to 200 nm and the cluster comprises ∼400 molecules in one dimension because the diameter of the mesogenic molecule is about 0.5 nm. Assume that the cluster form ratio is the same as for the LC molecules, i.e. ∼5, then the cluster length is ∼1 μm and the cluster comprises 0.6×10^8 mesogenic molecules. This number is by one or two orders of magnitude higher than the number of molecules in the cluster obtained by photoalignment [20]. Therefore the cluster length is 300–400 nm, its diameter is 65–85 nm (1/3 of the pore diameter) and the clusters' packing in the pore is of the hexagonal type. Semispherical pore is considered in the paper. Therefore its curvature radius is a parameter that characterizes the surface topology.

Other experiments with analog models demonstrated the planar type of the LC orientation if the LC does not interact with the micropore surface and the pore diameter is 1.5–2 times larger than the LC cluster size (∼ 1 μm).

For higher anchoring energy value ($\Delta G = 10^{-2}\text{J/m}^2$) the LC orientation in the micropores is planar and independent on their size. For intermediate values of ΔG the alignment is homeotropic for moderate pore diameter (up to 150 nm) and is tilted if the diameter of the pores is between 150 nm and 250 nm.

The alignment type is determined by the anchoring free energy which is expressed as

$$G_{pl} = H_{pl} - T S_{pl},$$
$$G_{\text{hom}} = H_{\text{hom}} - T S_{\text{hom}},$$

where G_{pl} and G_{hom} is the Gibbs free energy, H_{pl} and H_{hom} is the enthalpy and S_{pl} and S_{hom} is the entropy for planar and homeotropic alignment, respectively. Thus

$$\Delta G = G_{pl} - G_{\text{hom}} = H_{pl} - H_{\text{hom}} - T\left(S_{pl} - S_{\text{hom}}\right).$$

For $\Delta G < 0$ the orientation is planar, and for $\Delta G > 0$ the orientation is homeotropic. For small anchoring energy $H_{pl} \approx H_{\text{hom}}$ and thus the alignent type is determined by the orientation entropy. If $S_{pl} > S_{\text{hom}}$ the orientation is planar, and if $S_{pl} < S_{\text{hom}}$ the orientation is homeotropic. For both high and moderate anchoring energy the orientation type is determined by the orientation entropy because the difference of the energy of the LC interaction with the pore surface for both planar and hometropic orientation depends on the interaction of the molecules which are located close to the internal pore surface only. This difference is of the order of 1/100 of the total interaction between the molecules and the surface. For higher values of this difference the alignment would be homeotropic.

The entropy can be calculated using the lattice model. The clusters are oriented independently and entropy is determined by the Boltzmann formula:

$$S = k \ln W$$

where k is Boltzmann constant, and W is the number of microstates which corresponds to the given macrostate.

The number of microstates in the case of planar orientation is expressed as:

$$W_{pl} = \frac{\left(v_{pl} \cdot v_{pl}^0\right)!}{\left(v_{pl} \cdot v_{pl}^0 - N\right)! N!},$$

where N is the clusters number density ($N = N_A/n$), n is the number of mesogenic molecules in the cluster, v_{pl} is the number of micropores in one mole, and v_{pl}^0 is the number of the orienational states in the pore in the case of planar orientation.

In the case of homeotropic of alignment the placement number is given by:

$$W_{\text{hom}} = \frac{\left(v_{\text{hom}} \cdot v_{\text{hom}}^0\right)!}{\left(v_{\text{hom}} \cdot v_{\text{hom}}^0 - N\right)! N!},$$

where ν_{hom}– number of micropores per mole with homeotropic orientation, v_{hom}^0 is the number of the orienational states in the pore in the case of homeotropic orientation.

The molar entropy difference for planar and homeotropic orientation is equal to

$$\Delta S = S_{pl}\ S_{\text{hom}} = k \ln \frac{\left(v_{pl} v_{pl}^0\right)!\left(v_{\text{hom}} v_{\text{hom}}^0\ N\right)!}{\left(v_{\text{hom}} v_{\text{hom}}^0\right)!\left(v_{pl} v_{pl}^0\ N\right)!}.$$

Using the Stirling formula and the expansion $\ln(1 \pm x) = \pm x - \frac{x^2}{2} \pm \frac{x^3}{3}$: one obtains the following expression

$$\Delta S = kN\left(\ln\frac{v_{pl}^0}{v_{\text{hom}}^0} + \ln\frac{v_{pl}}{v_{\text{hom}}} - \frac{1}{2}\left[\frac{N}{v_{pl}\cdot v_{pl}^0} - \frac{N}{v_{\text{hom}}\cdot v_{\text{hom}}^0}\right] - \frac{1}{3}\left[\left(\frac{N}{v_{pl}\cdot v_{pl}^0}\right)^2 - \left(\frac{N}{v_{\text{hom}}\cdot v_{\text{hom}}^0}\right)^2\right]\right)$$

It can be shown that $\frac{N}{v_{pl}v_{pl}^0} << 1$, $\frac{N}{v_{\text{hom}}v_{\text{hom}}^0} \approx 1$ and $\frac{v_{pl}}{v_{\text{hom}}} \approx 1$, so

$$\Delta S \approx kN\ln\frac{\nu_{pl}^0}{\nu_{\text{hom}}^0}.$$

Then

$$\frac{T\Delta S}{A} = \frac{kN\ln\left(\nu_{pl}^0/\nu_{\text{hom}}^0\right)}{NA_0} = \frac{k\ln\left(\nu_{pl}^0/\nu_{\text{hom}}^0\right)}{A_0},$$

where A_0 and A – hemispherical values of cross-sectional area per one cluster and N clusters, respectively.

The model presented in this part enables one to calculate the thermodynamic parameters that determine the LC alignment. For the clusters with diameters presented in Part 2.2 a part of the free anchoring energy difference which is determined by the difference planar and homeotropic orientation entropies is equal to $10^{-6} \div 10^{-5} J/m^2$. It corresponds to low values of the free anchoring energy presented in Table 1.

Therefore the increase of the LC interaction with the micropores' surface results in an increase of the contribution of the clusters interaction with this surface and then to an increase of the anchoring energy.

4. Conclusions

A theory of the LC alignment in porous system is proposed for the first time that enables one to predict the alignment type and to explain the existing experimental data.

In the framework of this theory a dependence of the pore diameter on the fabrication conditions has been established and the effect of the minimum width of the alumina nanomesh on the pores' performances has been simulated. One concludes that the LC alignment type is determined by the LC clusters formation and by the ratio of their size and the pore size.

The mesogen orientation is determined the entropy difference between states with planar and homeotropic orientation.

A simple method of fabrication of the nanomesh alumina films for the LC alignment is presented and theoretical models which describe their structure and manufacturing process are developed.

Funding

This work was supported by the Russian Foundation for Basic Research (Grant No. 14-07-00574_a) and by the RF President's Grants Council (Support to Young Russian Scientists Program, Grant No. MK-2382.2014.9).

References

[1] Smirnov, A., Stsiapanau, A., Mohammed, A., Mukha, E., Kwok, H. S., Murauski, A. (2011). Proc. SID Symposium "Display Week-2011," 1385–1387.
[2] Bezborodov, V., Mikhalyonok, S., Zharski, I., Dormeshkin, O., Smirnov, A., Stsiapanau, A. (2013). 33rd International Display Research Conference EuroDisplay, 81–84.
[3] Lazarouk, S. K., Sashinovich, D. A., Katsuba, P. S., Smirnov, A. G., Astafjev, V. M. (2007). Proc. EuroDisplay, 32–34.
[4] Lazarouk, S., Muravski, An., Sashinovich, D. A., Chigrinov, V. G., Kwok, H. S. (2007). *Jpn. J. Appl. Phys.*, *46*, 6889–6892.
[5] Maeda, T., Hiroshima, K. (2004). *Jpn. J. Appl. Phys.*, *43*, L 1004–L 1006.
[6] Smirnov, A., Stsiapanau, A., Mukha, Y., Mazaeva, V., Belyaev, V. (2013). *SID Digest*, 1414.
[7] Stsiapanau, A., Smirnov, A., Yasyunas, A. (2012). 20th Advanced Display and Lighting Technologies Symposium, Ukraine, 37.
[8] Smirnov, A., Stsiapanau, A., Mukha, E. (2012). 20th Advanced Display and Lighting Technologies Symposium, Ukraine, 22.
[9] Smirnov, A., Poznyak, P., Stsiapanau, A. (2012). 20th Advanced Display and Lighting Technologies Symposium, Ukraine, 8.
[10] Stsiapanau, A., Smirnov, A., Satskevich, Y. (2012). 20th Advanced Display and Lighting Technologies Symposium, Ukraine, 7.
[11] Stsiapanau, A., Smirnov, A., Astafyev, V. (2012). 20th Advanced Display and Lighting Technologies Symposium, Ukraine, 24.
[12] Cognard, J. (1982). *Molecular Crystals and Liquid Crystals, Suppl. V.1* (Gordon and Breach, London).
[13] Palermo, V., Biscarini, F., Zannoni, C. (1998). *Physical Review E.*, *57*, 2519.
[14] Dadivanyan, A. K., Pashinina, Y. M., Chausov, D. N., Belyaev, V. V., Solomatin, A. S. (2011). *Mol. Cryst. Liq. Cryst.*, *545*, 159–167.
[15] Dadivanyan, A. K., Noah, O. V., Pashinina, Y. M., Belyaev, V. V., Chigrinov, V. G., Chausov, D. N. (2012). *Mol. Cryst. Liq. Cryst.*, *560*, 108–114.
[16] Dadivanyan, A. K., Chausov, D. N., Noah, O. V., Belyaev, V. V., Chigrinov, V. G., Pashinina, Y. M. (2012). *JETP*, *115*, 1100–1104.
[17] Ranjkesh, A., Ambrožič, M., Kralj, S., and Sluckin, T. J. (2014). 25th International Liquid Crystal Conference, Dublin, Ireland. 29th June – 4th July 2014. Abstracts, TM-O3.001.
[18] Dadivanyan, A. K., Belyaev, V. V., Chausov, D. N., Stsiapanau, A. A., Smirnov, A. G., Tsybin, A. G., Kurilov, A. D. (2014). SID Digest of Technical Papers, p.1374–1377.
[19] Dadivanyan, A. K., Belyaev, V. V., Chausov, D. N., Smirnov, A. G., Stsiapanau, A. A., Satskevich, Y.; Kurilov, A. D. (2014). *Zhidkie Kristally i ikh Prakticheskoye Ispolzovaniye (Liquid Crystals and Their Application in Praxis)*, No. *4* (46), 81–86.
[20] Kozenkov, V., Belyaev, V., Chigrinov, V., Tumovskii, G., Spakhov, A. (2012). *SID Digest*, 1411–1414.